Proton Exchange Composite Membranes from Blends of Brominated and Sulfonated Poly(2,6-dimethyl-1,4-phenylene oxide)

Tongwen Xu,[1,2] Dan Wu,[1,2] Seok-Jun Seo,[1] Jung-Je Woo,[1] Liang Wu,[1,2] Seung-Hyeon Moon[1]

[1]*Departmental of Environmental Science and Engineering, Gwangju Institute of Science and Technology, 1 Oryong-dong, Buk-gu, Gwangju 500712, Republic of Korea*
[2]*Department of Polymer Science and Engineering and Laboratory of Functional Membranes, School of Chemistry and Materials Science, University of Science and Technology of China, 96 Jinzhai Road, Hefei, Anhui 230026, People's Republic of China*

Received 29 August 2010; accepted 18 August 2011
DOI 10.1002/app.35494
Published online 21 November 2011 in Wiley Online Library (wileyonlinelibrary.com).

ABSTRACT: New composite proton exchange membrane was prepared by mixing a 1-methyl-2-pyrrolidone (NMP) solution of sulfonated poly(2,6-dimethyl-1,4-phenylene oxide) (SPPO) in sodium form and brominated poly(2,6-dimethyl-1,4-phenylene oxide) (BPPO) for hydrophilic-hydrophobic balance, then casting the solution as a thin film, evaporating the solvent, and treating the membrane with aqueous hydrochloric acid. The resulting membranes were subsequently characterized using FTIR-ATR, SEM-EDXA, and TGA instrumentation as well as measurements of basic properties such as ion exchange capacity (IEC), water uptake, proton conductivity, methanol permeability, and single cell performance. Water uptake, IEC, proton conductivity, and methanol permeability all increased with a corresponding increase of SPPO content. By properly compromising the conductivity and methanol permeability, membranes with 60–80 wt % SPPO content exhibited comparable proton conductivity to that of Nafion® 117, with only half the methanol permeability, thereby demonstrating higher single cell performance. The membranes developed in this study could thus be a suitable candidate electrolyte for proton exchange membrane fuel cells (PEMFCs). © 2011 Wiley Periodicals, Inc. J Appl Polym Sci 124: 3511–3519, 2012

Key words: fuel cells; proton exchange membrane; PEMFC; ionic conductivity; methanol permeability

INTRODUCTION

Proton exchange membrane fuel cells (PEMFCs) are of great interest as power sources in vehicles and portable applications because of their high energy efficiency and environmentally friendly features.[1,2] However, as PEMFC technology gains a significant share of the electrical power market, important issues such as optimal choice of fuel and development of alternative materials in the PEMFC stack have yet to be fully addressed.[3] Perfluorosulfonic acid polymers like Nafion® have some good properties for PEMFC applications and have been the industry and academic standard reference membrane for the last ten years, but they also have a number of drawbacks that need to be overcome, such as its high cost due to its complicated manufacturing procedure, high methanol permeability, and poor performances at elevated temperatures.[4–7] These factors have limited its commercial applications; thus, there is a strong desire to find new proton exchange membranes (PEMs) that can achieve high performances at a low cost. To this end, the most viable alternative is to develop a nonfluorinated membrane,[5–7] as blends of nonfluorinated polymer materials can potentially provide a very cheap and convenient route for proton-exchange membranes.[7–15] At a minimum, such blends should contain a proton conducting sulfonated aromatic polymer and a binder. To date, a number of blend membranes have been reported including sulfonated poly(ether sulfone) (SPES), sulfonated polysulfone (SPS), sulfonated poly(ether-ether ketone) (SPEEK), sulfonated poly(2,6-dimethyl-1,4-phenylene oxide) (SPPO), etc.,[7–16] while others have focused on the binders including epoxy resin,[8] imidazole,[9] polybenzimidazole (PBI),[10] and polyvinylidene fluoride (PVDF),[11] or inorganic materials such as boron phosphate,[12] and inorganic nanoparticles.[13]

For fuel cell membranes constructed from polymer blends, it is quite important to control the physical hydrophilic–hydrophobic balance in the morphology. It has been widely accepted that the hydrophilic

Correspondence to: S.-H. Moon (shmoon@gist.kr.ac).
Contract grant sponsor: Joint Research Project (KOSEF-NSFC Cooperative Program); contract grant numbers: F01-2009-000-10171-0, 20911140273, 20911140273.
Contract grant sponsor: Natural Science Foundations of China; contract grant number: 20974106.

domain facilitates the transport of water and methanol, while the hydrophobic domain inhibits their movements but offers good mechanical strength against swelling.[16] In addition, there have been reports stating that PEM fabrications for direct methanol fuel cell (DMFC) can be achieved through the optimal mixing of the two parts in membranes by forming acid–base complex blends[9,17] or hydrophilic–hydrophobic balanced block copolymers.[18] However, in most cases, the functional polymers (hydrophilic part) and the binder (hydrophobic part) are of completely different structures and chemistry resulting in limited compatibility or miscibility.[9–14]

Among engineering plastics, poly(2,6-dimethyl-1,4-phenylene oxide) (PPO) is considered a very hydrophobic polymer with very high glass transition temperature (T_g = 212°C) and hydrolytic stability.[19] Specifically, the corresponding sulfonated materials (i.e., SPPO) have been considered as good proton-exchange materials with high thermal stability, despite the fact that its dimensional instability prevents it from practical applications in fuel cells.[20–23] However, although PPO is a very simple structure compared with other aromatic polymers, it can easily conduct polymer analogous reactions in both aryl- and benzyl-positions, such as electrophilic substitution on the benzene ring of PPO, radical substitution of hydrogen from the methyl groups of PPO, nucleophilic substitution of brominated PPO, capping and coupling reactions of the terminal hydroxyl groups of PPO chains, and metalation of PPO with organometallic compounds.[24–28] Scheme 1 shows the chemical structures of PPO, SPPO, and brominated PPO containing both aryl and benzyl substitutions, which were used in this work. It can thus be expected that these substituted materials have good miscibility due to the presence of the same PPO backbone. Therefore, to increase the mechanical stability of SPPO and determine the optimum miscible blend, new composite membranes from blends of SPPO and brominated PPO will be prepared in this article, and their structures and fundamental properties will be subsequently discussed in terms of their relative contents.

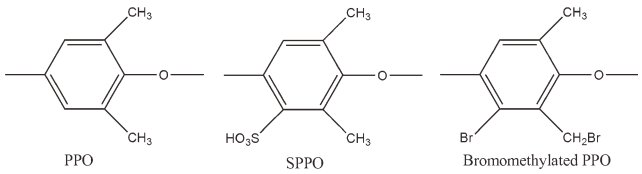

Scheme 1 The chemical structures of PPO, SPPO and brominated PPO used in this work.

EXPERIMENTAL

Materials

For this study, PPO, M_w = 48,000 g mol^{-1} and M_w/M_n = 2.7, was commercially obtained from the Institute of Chemical Engineering, Beijing (China), and SPPO was obtained from the TianWei Membrane Corporation, Shandong (China). For the SPPO, the IEC was experimentally verified by the authors, at a value of 2.37 meq g^{-1} (sulfonation degree about 37.5%). Bromine supplied by the Shanghai Chemical Reagent Co. was used for the preparation of brominated PPO. Note that solvents such as chlorobenzene, methanol, and 1-methyl-2-pyrrolidone (NMP) are all of analytical grade, and were used as received.

Bromination of PPO

Bromination of PPO was achieved according to the method described in our previous article.[27] In brief, 12 g of PPO was dissolved in chlorobenzene to form an 8 wt % solution, and this solution was then subjected to bromination at its boiling point (130–132°C) by adding 16 g of bromine diluted with chlorobenzene to obtain a brominated PPO (BPPO) solution. This solution was subsequently precipitated with methanol, washed, and dried at 80°C for one day to produce a substituted brominated polymer. Ensuing ^{1}H-NMR (Unity plus 400) measurements showed that BPPO has 29% aryl-substitution and 73% benzyl substitution.

Preparation of composite membranes

BPPO and SPPO in sodium form were dissolved separately in NMP to produce a homogenous solution with concentrations of 27.3 wt % and 22.2 wt %, respectively. The blend membrane was prepared by casting the mixture solution of SPPO and BPPO in a clean glass dish, and allowing the solvent evaporate at 80°C under strong air flow for 4 h, then being dried at 60°C for another 24 h. In this study, the blend ratio is calculated as the ratio of SPPO for the total polymers without considering the solvent. For example, if a blend membrane of 10 wt % SPPO was prepared, the casting solution would contain 10 g SPPO (from 10/0.222 g SPPO solution) and 90 g BPPO (from 90/0.273 g BPPO solution). The dried film with a thickness of about 40 μm was removed from the glass plate by immersing it into a deionized water bath; the resulting membrane was washed by deionized water for several times and immersed into 1*M* aqueous HCl for 24 h, and then again washed in deionized water.

Instruments

Fourier transform infrared spectra (FTIR) of the prepared membranes were measured by a Jasco 460 plus spectrometer (Tokyo, Japan) for the characteristic

groups. Thermal behavior of the sulfonated membranes was determined by thermogravimetric analysis (TGA) on a Shimadzu TGA-50H analyzer in nitrogen gas flushed at 20 mL min^{-1}, at a heating rate of 10°C min^{-1}. Both the surface and cross section morphology of the membranes were observed using the field emission scanning electron microscopy (XT30 ESEM-TMP PHILIP), and the distributions of C, O, and S atoms in the thickness direction were analyzed through energy-dispersive x-ray analysis (EDXA).

Conductivity measurements

A four-point probe method using a lab-made cell consisting of two platinum plates carrying the current and two platinum wires monitoring the potential drop was employed to measure the proton conductivity of the membranes. The impedance was determined using an Autolab PGSTAT 30 (Eco Chemie, Netherland) in galvanostatic mode at an alternating current (AC) with amplitude of 0.1 mA over a frequency range of 1 MHz to 50 Hz at room temperature. The frequency region over which the impedance had a constant value was measured using a Bode plot, and the resistance was then obtained from a Nyquist plot. Here, the proton conductivity (κ) was calculated according to the expression

$$\kappa = \frac{L}{RWd} \tag{1}$$

where R is the obtained membrane resistance, L is the distance between potential-sensing electrodes (here 1 cm), and W and d are the width (here 1 cm) and thickness of the membrane, respectively. During measurement, the membrane was fully hydrated at room temperature and the data were determined through three independent measurements, and the uncertainty with conductivity values was estimated to be approximately ±5%.

Water uptake, ion exchange capacity, and dimensional stability

The membrane in H^+ form was soaked in distilled water at room temperature for 24 h. After complete swelling, the sample was removed and excess water adhering to the surface was quickly wiped with a tissue paper. The weight in a wet state was measured using an electronic balance (Advanture™; readability 0.0001 g), and the membrane in H^+ form was then soaked in 0.5 mol L^{-1} NaCl solution at room temperature for 24 h. After removing the membrane, the solution was titrated using a 0.01 mol L^{-1} NaOH standard solution with a drop of phenolphthalein solution (1% in ethanol) as the pH indicator. The membrane sample was subsequently converted into acid form using 1 mol L^{-1} HCl and washed in deionized water to remove any free acid. Finally, the sample was dried at 50°C under a vacuum for 24 h and the dry weight measured. The experimental water uptake (W_R) and IEC could then be calculated as

$$W_R = \frac{w_{\text{wet}} - w_{\text{dry}}}{w_{\text{dry}}} \times 100\% \tag{2}$$

$$\text{IEC} = \frac{C_{\text{NaOH}} \cdot V_{\text{NaOH}}}{w_{\text{dry}}} \tag{3}$$

where w_{wet} and w_{dry} are the wet and dry weights of the sample, respectively, and C_{NaOH}, V_{NaOH} are the concentration and volume of the NaOH solution, respectively.

The dimensional stability defined by the linear expansion ratio (LER) was determined based on the difference between the wet and dry dimensions of the membranes, which were cut into 1 cm × 3 cm and calculated as

$$\text{LER} = \frac{L_{\text{wet}} - L_{\text{dry}}}{L_{\text{dry}}} \times 100\% \tag{4}$$

where L_{wet} and L_{dry} are the widths of the membrane in wet state (in distilled water at room temperature for 24 h) and dry state (under vacuum at 50°C for 24 h), respectively.

Methanol permeability

The methanol permeability was measured using a lab-made two-compartment measuring cell with a 1.0 cm diameter hole for diffusion; the procedure has been described in detail elsewhere.[29] One compartment was filled with a 150 mL 20 % (v/v) methanol aqueous solution, and the other with deionized water of equal volume. The methanol concentration in the deionized water compartment was monitored on-line using a refractive index detector (RI750F, Younglin Instrument, Korea), driven by a Masterflex pump through a 1 mm diameter silicon tube at a constant speed of 1.0 mL min^{-1}. The output signal was then converted with a data module (Autochro, Younglin Instrument, Korea) and recorded on a personal computer. For each test, the time was set at 40 min to ensure linearity of the diffusional curves. The methanol permeability (P) was obtained using

$$P = kV_B d/(C_{A0}.A) \tag{5}$$

where C_{A0} is the initial methanol concentration (C_{A0}= 20% v/v), k is the slope of the linear part of the diffusional curve, V_B is the volume of deionized water in the water compartment, d is the membrane thickness, and A is the effective permeation area. For

comparison, Nafion® 117 was tested under the same experimental conditions.

Single cell performance[30]

A blend proton exchange membrane with 80 wt % SPPO content was selected as an example to evaluate PEMFC performance. Here, gas diffusion layers (GDL; SIGRACET®) were coated with Pt/C catalyst slurry (40 wt % Pt) using a spray gun, and loading of the Pt catalyst was 0.4 mg cm^{-2}. The membrane-electrode assembly (MEA) was prepared by directly sandwiching the membrane between two sheets of GDL without hot-pressing; the MEA was then set into a fuel cell station with an effective area of 5 cm^2. The test was conducted under atmospheric pressure with a cell temperature of 50°C, and both the flow rate of the fuel for the anode (pure hydrogen) and oxidant for the cathode (pure oxygen) were 150 mL min^{-1}, respectively; hydrogen and oxygen were pre-bubbled in distilled water at 55°C to introduce humidity. The current-voltage (I-V) performance of the cell was subsequently recorded at a descending voltage rate of 0.02 V s^{-1} using an electronic loader. Note that for comparison, Nafion® 117 was tested under the same experimental conditions.

RESULTS AND DISCUSSION

FTIR

Figure 1 presents the FTIR spectra for blend membranes with different SPPO contents. For simplicity, the figure only shows the spectra of membranes with SPPO contents of 8.3 wt %, 16.9 wt %, 44.9 wt %, and 90 wt %; spectra for the other blend membranes follow similar trends. These FTIR spectra illustrate the appearance of absorption peaks of C—O (ether bonds), phenyl group, and C—Br bonds in BPPO materials. Previously, symmetrical and asymmetrical stretching vibrations of C—O (Ph—O—C) and phenyl group have been known to appear at 1050 cm^{-1} and 887 cm^{-1}, 1205 cm^{-1}, 1466 cm^{-1}, 1603 cm^{-1}, and 2953 cm^{-1} for different substitutions; the peaks near 500–600 cm^{-1} correspond to C—Br bonds.[24,27,31] Evidence of SPPO appears at 675 cm^{-1} and 1030 cm^{-1}, peaks assigned to the symmetric and asymmetric stretching of sulfonated acid groups. The differences between blend membranes with varying SPPO contents can be judged from the peaks at 3444 cm^{-1} and 1204 cm^{-1}. The former corresponds to the symmetrical and asymmetrical stretching vibration bonds of O—H vapor, and the latter to the interaction between sulfuric groups and water vapor. Obviously, with an increase in SPPO content, the intensity of these two bonds increases correspondingly. Indeed, there is remarkable increase in peak density when the SPPO content changes from 16.9 wt % to 45 wt %. As will be discussed later, this point corresponds to the transition from insulator to conductor of the composite membranes.

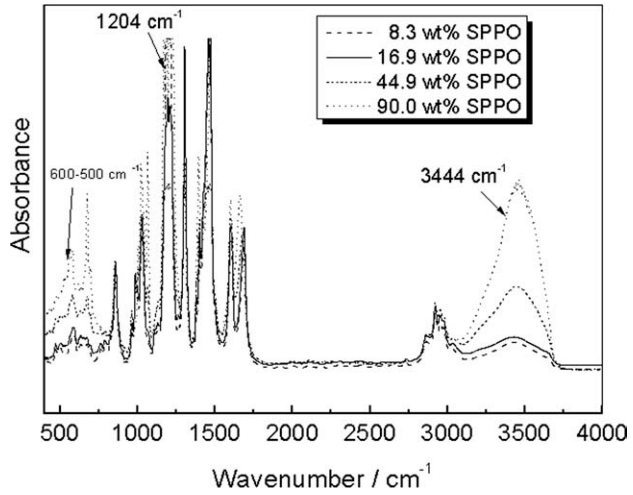

Figure 1 FTIR spectra of BPPO/SPPO blend membranes with different SPPO content (8.3, 16. 9, 44.9, and 90 wt %).

Thermal stability

The thermal stabilities, as a function of weight loss ratio, were evaluated via TGA at a heating rate of 10°C min^{-1} under nitrogen [Fig. 2(a)], with the corresponding weight loss peaks shown in Figure 2(b). It was observed that the thermal degradation behaviors for all the blend membranes are divided into four stages. The initial weight loss occurring at around 50°C is ascribed to water in the membranes. This loss increases with an increase in SPPO content, thereby indicating the hygroscopic nature of blend membranes with high SPPO content. The peaks appearing at 320 and 450°C are respectively caused by decomposition of the methyl and ether groups of BPPO or SPPO, and the splitting of residue of BPPO or SPPO, respectively[31]; deduced from BPPO curves, which only show these two peaks.

The peak at 210°C for the blend membranes may be caused by decomposition of the sulfuric groups and the residual solvent such as NMP (b.p. 204°C). As can be calculated from Figure 2(a), weight loss in the range of 150–250°C for the pure BPPO membrane is 1.41 wt %, whereas the ratios of weight loss for blend membranes with 8.3, 44.9, and 65.5 wt % SPPO contents were 9.13, 9.76, and 9.42 wt %, respectively. As the NMP has high affinity with $-SO_3H$ groups, the residual NMP content in the membranes will generally increase simultaneously. Even taking this factor into consideration, the general increasing trend is attributed to the increasing $-SO_3H$ contents in the membranes. Therefore, the result confirms that the thermal stability of the blend

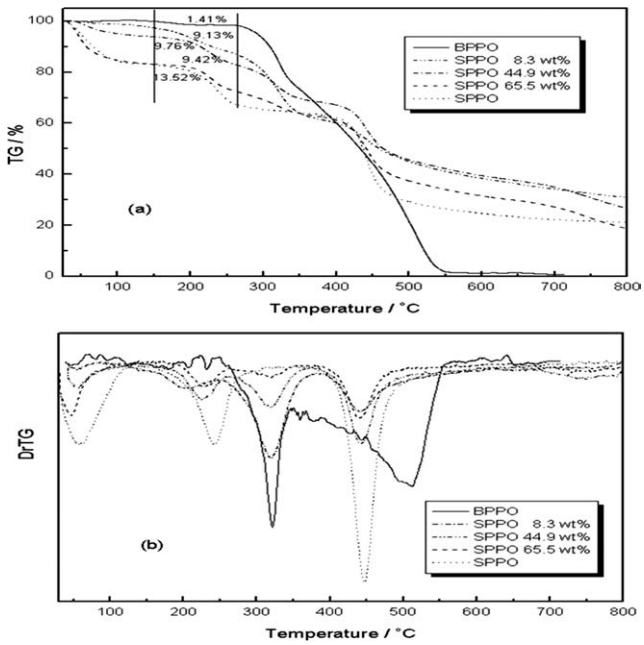

Figure 2 (a) TGA and (b) DrTGA curves of BPPO/SPPO blend membranes with different SPPO content.

membrane is largely dependent on SPPO, and that no chemical bond has formed in the blends. Note that the ratio of weight loss for the pure SPPO membrane determined at the identical conditions is 13.52 wt %; thus, an incorporation of BPPO into SPPO can potentially increase the thermal stability of the blend membranes.

Morphology

The membrane surface morphology was observed using the field emission scanning electron microscopy, the results of which are shown in Figure 3 for samples with SPPO contents ranging from 8.3 to 90 wt %. Obviously, the morphology of the surface, particle size, and distribution were all strongly affected by the relative content of the blend. From the figures, it can be seen that the homogeneity of the blend membranes decreases with SPPO contents, and then increases at higher content levels. For example, membranes prepared from low SPPO content (8.3 wt %) or high SPPO content (>65.5 wt %) show high surface uniformity; whereas the membranes prepared from medium contents of SPPO such as in Figure 3(c) (44.9 wt % SPPO) and Figure 3(d) (65.5 wt % SPPO) show macro-phase separation. Especially, the maximum particle size can be seen when the SPPO content is close to that of BPPO. For an example, as shown in Figure 3(c); the average particle size for sample with 44.5 wt % SPPO is greater than 100 μm. Strangely, this size was larger than the practical membrane thickness (40 μm). The main reasons are that at this composition the membrane surface is very rough due to phase separation and also the particles are not definitely spheric. A further elemental analysis using EDXA shows that the size of these particles is mainly due to SPPO. Therefore, from the percolation concept,[32] as long as the particles form a minimum connection required for effective conductance (above the percolation threshold), they do not affect any of the blend membranes as proton conductors. Thus, in terms of homogeneity, a blend membrane with above 65 wt % SPPO is suitable for fuel cell applications.

To have a direct view of the microstructure of the blend membranes, SEM-EDXA was used to display the membrane's vertical section. The distributions of Br and S atoms, representative atoms for the respective polymers, were simultaneously recorded in the thickness direction. Our preliminary tests show that different blends demonstrate different main element distributions, and also that all the distributions seem uniform. Figure 4 shows a sample with 65.5 wt % with SPPO content, where it can be clearly seen that the distributions of these elements are nearly uniform in the thickness direction. These results are consistent with the corresponding surface images [Fig. 3(c)].

Water uptake, ion exchange capacity, and proton conductivity

Figure 5 demonstrates the measured membrane water uptake and IEC. All samples show a reasonable trend; both the IEC and water uptake increase nearly linearly with respect to the SPPO content. This linear increase occurs as only SPPO contributes to the functional groups and the BPPO matrix acts as an inert matrix due to its hydrophobic nature. Compared with the pure SPPO membrane with a water uptake of about 80%, the blend membrane has a significantly lower water uptake, thereby exhibiting better dimensional stability.

Theoretical IEC is also calculated based on the wt % of SPPO in the blends, the results of which as shown in Figure 5 are in a comparison with the experimental values. It is well known that if the blend forms an acid–base complex, the theoretical IEC will be different from the experimental values.[33] In our case, the theoretical IEC is relatively consistent with the experimental values, suggesting that there is no chemical interaction between BPPO and SPPO.

The conductivities of the blend membranes for varying SPPO contents are shown in Figure 6. It is interesting to note that a percolation threshold exists at around 20 wt % SPPO; below which the conductivity of the blend membrane is negligible, and above which the membrane has a sudden increase in proton conductivity. Such trends have been previously observed in other insulator-conductor

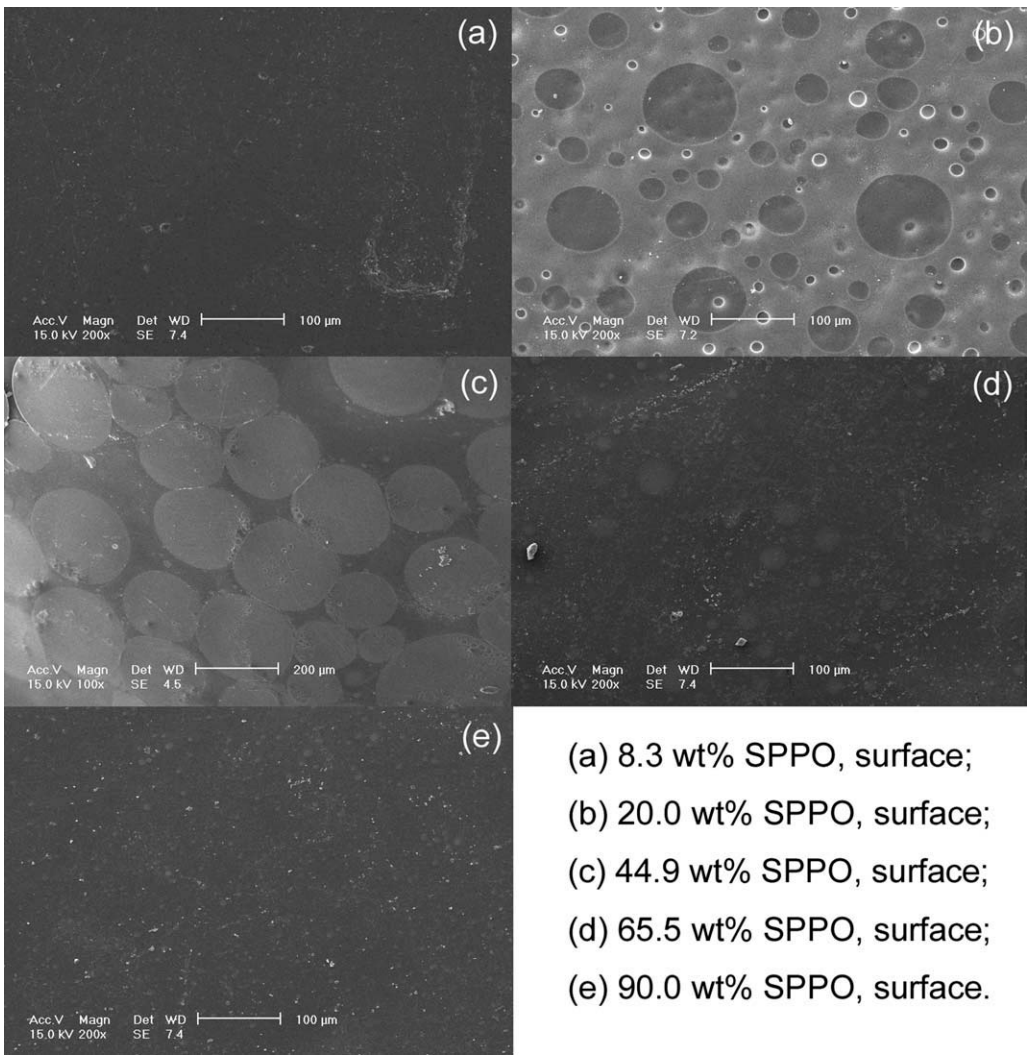

Figure 3 The surface SEM observation of the BPPO/SPPO blend membranes with different SPPO content.

transition systems, especially in SPPO matrix systems,[34] in which a percolation threshold value of about 18% was estimated. Very good conductivities are also observed for membranes containing greater than 60 wt % of SPPO. Specifically, when the SPPO content reaches as high as 70 wt %, the conductivity is above 0.08 S cm^{-1}, comparable with that of Nafion® 117 under the same conditions. Thus, the optimum SPPO content can be determined as 60–80 wt %, based on the conductivity value, methanol block, and dimensional stability, which will be further discussed in the following sections.

Methanol permeability

Gas crossover in fuel cells usually results in inefficient fuel utilization, mixed electrochemical potentials, and other specific operational problems. The extensive diffusion of hydrogen from the anode to the cathode may lead to the reduction of the available oxygen surface concentration at the catalyst/membrane interface because of the direct reaction of hydrogen with oxygen. Methanol crossover in DMFC occurs based on the similar principle. Therefore, the methanol permeability, measured conveniently by refractive index in aqueous solution, can be a characteristic membrane performance in fuel cells from the viewpoint of fuel leakage through membranes. Figure 7 shows the methanol permeability of the blend membranes. The methanol concentration used in these experiments was 20% (v/v). It can be seen that the methanol permeability increases with an increase in SPPO content in the blend membrane. The change is considerable at the SPPO content of 20 wt % where methanol permeability shows a sudden increase from 2.01×10^{-7} cm^2 s^{-1} to 5.79×10^{-7} cm^2 s^{-1}. This is similar to the conductivity dependence with a sudden increase at the same SPPO content (Fig. 6). Compared with Nafion® 117, which has a methanol permeation value of 2.14×10^{-6} cm^2 s^{-1} determined under identical conditions, all the blend membranes show noticeably less methanol permeability. Specifically, the

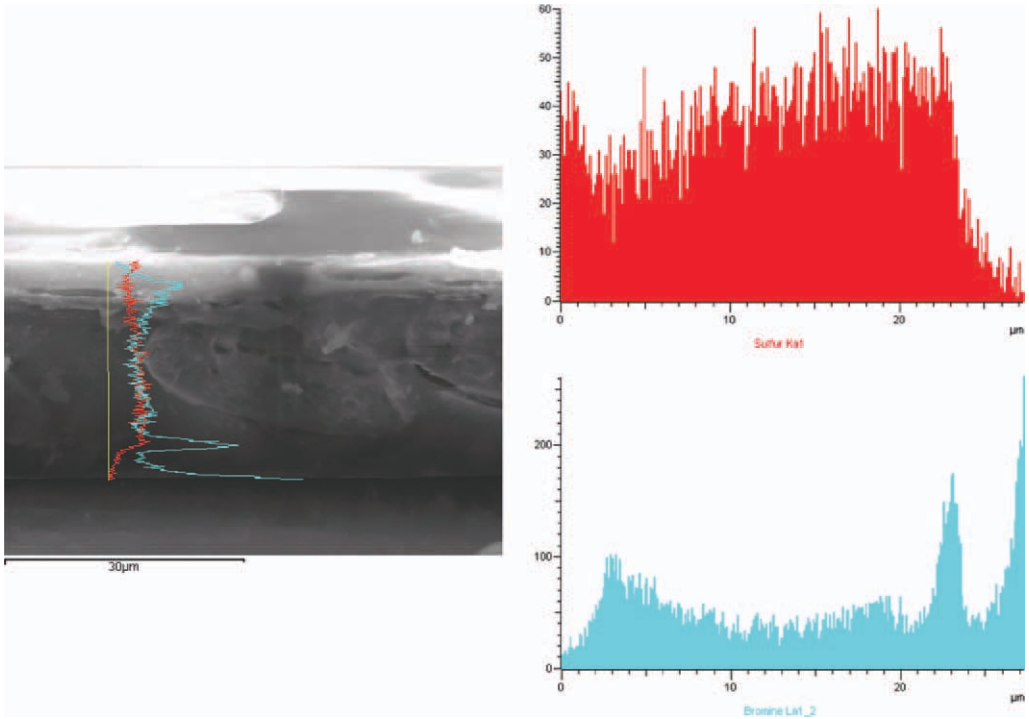

Figure 4 SEM-EDAX observation of BPPO/SPPO blend membranes (cross section) with 65.5 wt % SPPO. [Color figure can be viewed in the online issue, which is available at wileyonlinelibrary.com.]

block of methanol in membranes with 60–80 wt % SPPO, having comparable proton conductivity to Nafion® 117, was up to 2 times higher than that of Nafion® 117. It is possible that improvements in the methanol barrier may be related to the two important factors: one is that the hydrophobic bromines at the pendant of the BPPO backbone block the methanol diffusion and the other is the poor methanol affinity of backbone with the structure of phenylene-oxide (c.f. Scheme 1). The former was approved by our previous study, in which the membrane directly sulfonated from BPPO (not BPPO/SPPPO blends) showed extremely low methanol permeability, especially at the case of low sulfonation degrees.[35] The latter was confirmed by the job of Cho et al. It was reported that membranes prepared from a brominated poly(2,6-dimethyl-1,4-phenylene oxide)-*g*-poly (styrenesulfonic acid) (PPO-*g*-PSSA) graft copolymer had very low methanol permeability, with a magnitude of 10^{-7} cm^2 s^{-1}, and this value decreased with an increase in BPPO graft.[36] Though in this case, brominated PPO is used as a macro-initiator for grafting sodium styrene sulfonated on to PPO via living free radical polymerization and increasing BPPO results in greater graft content but the resulting polymer would not contain appreciable amounts

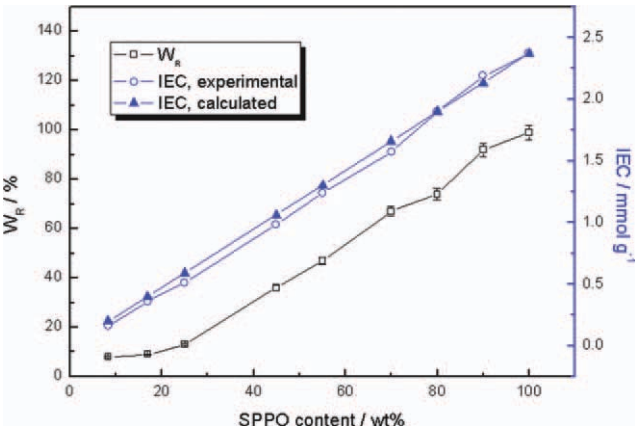

Figure 5 Effect of SPPO content on IEC and water uptake of blend membranes. [Color figure can be viewed in the online issue, which is available at wileyonlinelibrary.com.]

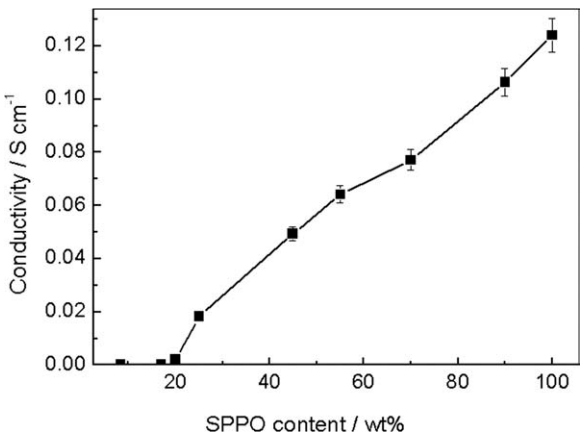

Figure 6 Effect of SPPO content on the conductivity of blend membranes.

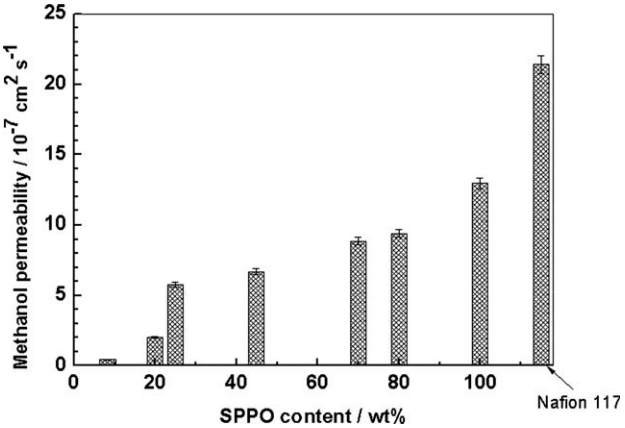

Figure 7 Effect of SPPO content on the methanol permeability of blend membranes in comparison with Nafion 117.

of bromine. Therefore, it can be concluded that a decrease in methanol permeability is attributed to an increase with structure of phenyleneoxide (PPO chain) because sodium styrene sulfonated has strong affinity to methanol.

Dimensional stability

The dimensional stability was measured as a linear change ratio in which the membrane was cut into 1 cm × 3 cm. From the Figure 8, it can be seen that the dimensional change ratio follows nearly the same trend as for other parameters such as proton conductivity and water uptake. As mentioned above, hydrophilic SPPO plays a decisive role in these water uptakes and with an increase in SPPO content, dimensional stability decreases due to an increase in water uptake. Hence, membranes with SPPO content below 25 wt % have high dimensional stability and a linear expansion ratio below 5%; those with 40–60 wt % SPPO have a close linear expansion ratio to

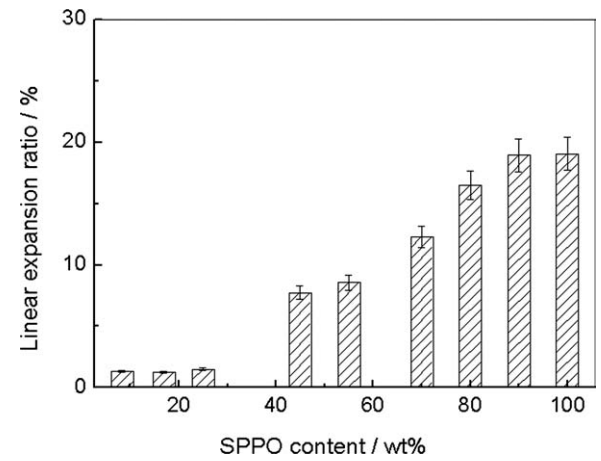

Figure 8 Effect of SPPO content on the linear expansion ratio (%) of the blend membranes.

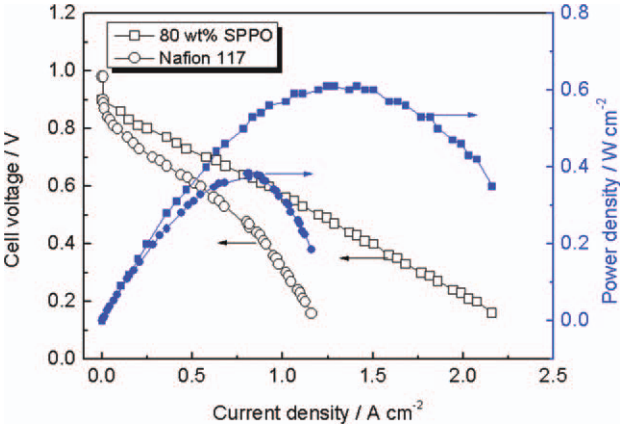

Figure 9 Comparison of polarization curves of the single cell tests between Nafion®117 (○) and the blend membrane with 80 wt % SPPO (□). Open symbols show cell voltage and the filled symbols show power density. [Color figure can be viewed in the online issue, which is available at wileyonlinelibrary.com.]

Nafion® 117, which has a value of 10.1% determined under the identical conditions. Membranes with 60–80 wt % SPPO have a relatively higher linear expansion ratio than Nafion® 117, though it is deemed acceptable because the linear expansion ratios were below 20%.

Single cell performance

A blend membrane with 80 wt % SPPO content was used to evaluate the PEMFC performance. As discussed above, the main properties of such membranes are: IEC = 1.9 mmol g^{-1}, Wr = 0.74 g water/g-dry membrane, thickness = 40 μm, linear expansion ratio = 16.51%, and methanol permeability = 9.41 × 10^{-7} cm^2 s^{-1}. The single cell employing the membrane was fed with humidified pure hydrogen and oxygen to the anode and cathode, respectively, and was operated at 50°C under atmospheric pressure. After the cell reached stable conditions (about 14 h), the current-voltage (I-V) performance of the cell was recorded as shown in Figure 9. For comparison, Nafion® 117 was also tested under the same conditions.

As shown in Figure 9, the open circuit voltage (OCV) of the blend membrane (900 mV) is slightly lower than that of Nafion® 117 (980 mV); it has been previously described that the OCV of PEMFC is dependent on the membrane permeance, rather than the permeability itself.[16,37] The permeance, which is the permeability divided by the membrane thickness, increases with a corresponding decrease in thickness. From the figure, though the blend membrane shows low methanol permeability, its thickness is around 40 μm, about 20 % of that of Nafion® 117 (around 200 μm). Therefore, the blend membrane shows

higher methanol permeance (2.35×10^{-4} cm s^{-1}) than Nafion®117 (1.12×10^{-4} cm s^{-1}) when thickness is considered. This may be the main reason why the blend membrane has a relatively lower OCV. However, as current density increases, the cell voltage in Nafion® 117 decreases more rapidly than that in the blend membranes.

It can also be observed that the maximum power density of the blend membrane with 80 wt % SPPO is about 610 mW cm^{-2} at 1288 mA cm^{-2}. This value is much higher than that of Nafion®117, which shows its highest power density of about 380 mW cm^{-2} at 820 mA cm^{-2}.[30] In addition, the current density of Nafion® 117 at the voltage of 0.6 V was about 550 mA cm^{-2}, whereas that for the blend membrane was about 928 mA cm^{-2}—nearly two times that of Nafion® 117. Although the values for Nafion®117 are somewhat lower than those of the commercial MEA,[38] having completely optimized preparation conditions, the MEA preparation procedure for Nafion® 117 and the blend membrane were the same in this study. Thus, from the performance of both cell voltage and power density, it can be confirmed that the blend membranes are quite comparable to Nafion® 117 membranes, and have high potential for use as an electrolyte for PEMFC.

CONCLUSIONS

A new composite membrane for potential fuel cell applications was prepared by blending SPPO and BPPO, based on the same base polymer PPO. In this composition, SPPO increased the membrane conductivity and water uptake while BPPO contributed to the dimensional stability and methanol barrier properties.

As expected, water uptake, IEC, proton conductivity, and methanol permeability all increased with a corresponding increase in SPPO content. Thus, by properly compromising the conductivity and methanol permeability, blend membranes with 60–80 wt % SPPO are potentially good candidates for DMFC or PEMFC membranes. Such membranes show comparable proton conductivity to that of Nafion® 117, though with only half the methanol permeability. Furthermore, based on SEM observations, the blend membranes in this SPPO range show a highly uniform structure.

The performance of a single cell for a sample blend membrane with 80 wt % SPPO was subsequently tested and compared with Nafion® 117 under identical conditions. The results of this test showed that the blend membrane has a relatively high cell voltage and power density compared to Nafion® and may provide potential applications in low temperature PEMFCs.

The authors express our high appreciation to Dr. C.M. Wu for experimental assistance and useful discussions.

References

1. Costamagna, P.; Srinivasan, S. J Power Sources 2001, 102, 242.
2. Carrette, L.; Friedrich, K. A.; Stimming, U. Chemphyschem 2000, 1, 162.
3. Steele, B. C. H.; Heinzel, A. Nature 2001, 414, 345.
4. Smitha, B.; Sridhar, S.; Khan, A. A. J Membr Sci 2005, 259, 10.
5. Hickner, M. A.; Ghassemi, H.; Kim, Y. S.; Einsia, B. R.; McGrath, E. Chem Rev 2004, 104, 4587.
6. Rozière, J.; Jones, D. J. Ann Rev Mater Res 2003, 33, 503.
7. Rikukawa, M.; Sanui, K. Prog Polym Sci 2000, 25, 1463.
8. Fu, T.; Zhao, C. J.; Zhong, S. L.; Zhang, G.; Shao, K.; Zhang, H. Q.; Wang, J.; Na, H. J Power Sources 2007, 165, 708.
9. Liu, Y. F.; Yu, Q. C.; Yuan, J.; Ma, L. L.; Wu, Y. H. Eur Polym J 2006, 42, 2199.
10. Daletou, M. K.; Gourdoupi, N.; Kallitsis, J. K. J Membr Sci 2005, 252, 115.
11. Mokrini, A.; Huneault, M. A. J Power Sources 2006, 154, 51.
12. Krishnan, P.; Park, J. S.; Kim, C. S. J Membr Sci 2006, 279, 220.
13. Anilkumar, G. M.; Nakazawa, S.; Okubo, T.; Yamaguchi, T. Electrochem Commun 2006, 8, 133.
14. Chang, J. H.; Park, J. H.; Park, G. G.; Kim, C. S.; Park, O. O. J Power Sources 2003, 124, 18.
15. Iojoiu, C.; Marechal, M.; Chabert, F.; Sanchez, J. Y. Fuel Cells 2005, 5, 344.
16. Jung, B.; Kim, B.; Yang, J. M. J Membr Sci 2004, 245, 61.
17. Kerres, J. A. Fuel Cells 2005, 5, 230.
18. Kim, J.; Kim, B.; Jung, B.; Kang, Y. S.; Ha, H. Y.; Oh, I.; Ihn, K. J. Macromol Rapid Commun 2002, 23, 753.
19. Pan, Y.; Huang, Y. H.; Liao, B.; Cong, G. M. J Appl Polym Sci 1996, 61, 1111.
20. Li, C. H.; Liu, J. H.; Guan, R.; Zhang, P. X.; Zhang, Q. L. J Membr Sci 2007, 287, 180.
21. Lu, D. P.; Lu, W.; Li, C. H.; Liu, J. H.; Xu, J. Solid State Ionics 2006, 177, 13.
22. Yang, S. F.; Gong, C. L.; Guan, R.; Zhou, H.; Dai, H. Polym Adv Technol 2006, 17, 360.
23. Kosmala, B.; Schauer, J. J Appl Polym Sci 2002, 85, 1118.
24. Liska, J.; Borsig, E. Chem Listy 1992, 86, 900.
25. Story, B. J.; Koros, W. J. J Membr Sci 1992, 67, 191.
26. Schauer, J.; Bleha, M. J Appl Polym Sci 1992, 46, 1807.
27. Wu, L.; Xu, T. W.; Yang, W. H. J Membr Sci 2006, 186, 185.
28. Xu, T. W.; Yang, W. H. J Membr Sci 2001, 190, 159.
29. Woo, Y.; Oh, S. Y.; Kang, Y. S.; Jung, B. J Membr Sci 2003, 220, 31.
30. Fu, R. Q.; Woo, J. J.; Seo, S. J.; Lee, J. S.; Moon, S. H. J Membr Sci 2007, 309, 156.
31. Zhang, S. L.; Wu, C. M.; Xu, T. W.; Gong, M.; Xu, X. L. J Solid State Chem 2005, 178, 2292.
32. Shante, V. K. S.; Kirkpatric, S. Adv Phys 1971, 20, 325.
33. Kerres, J.; Ullrich, A.; Meier, F.; Häring, T. Solid State Ionics 1999, 125, 243.
34. Xu, T. W.; Yang, W. H.; He, B. L. Chem Eng Sci 2001, 56, 5343.
35. Wu, D.; Fu, R. Q.; Xu, T. W.; Wu, L.; Yang, W. H. J Membr Sci 2010, 310, 522.
36. Cho, C. G.; Jang, H. Y.; You, Y. G.; Li, G. H.; An, S. G. High Perform Polym 2006, 18, 579.
37. Ren, X.; Wilson, M. S.; Cottesfeld, S. J Electrochem Soc 1996, 143, 11.
38. DuPont fuel cells, can be found under www.dupont.com/Fuel_Cells/en_US/products/mea.html, 2009.